ENOC-2008, Saint Petersburg, Russia, June, 30–July, 4 2008

FREE DYNAMICS OF FINITE CHAINS OF WEAKLY NONLINEAR OSCILLATORS

Francesco Romeo
Dipartimento di Ingegneria Strutturale e Geotecnica
Università di Roma La Sapienza
Italy
francesco.romeo@uniroma1.it

Giuseppe Rega
Dipartimento di Ingegneria Strutturale e Geotecnica
Università di Roma La Sapienza
Italy
giuseppe.rega@uniroma1.it

Abstract
Infinite and finite chains of mono-coupled nonlinear oscillators are considered. The dynamics of these one dimensional chains is studied relying upon discrete nonlinear periodic models governed by second order nonlinear difference equations. At first, amplitude dependent frequency thresholds bounding nonlinear propagation and attenuation zones are determined for infinite chains through a nonlinear map approach. Next, finite chains with homogenous boundary conditions are tackled through the multiple scales perturbation approach by assuming weak nonlinearities. Free vibrations frequency-amplitude curves as well as nonlinear modes are determined. Furthermore, their connection with the amplitude dependent frequency thresholds of the nonlinear propagation zone is discussed.

Key words
Nonlinear periodic structures, wave propagation, multiple scales, nonlinear frequencies and modes.

1 Introduction

The dynamics of one dimensional chains of linearly coupled nonlinear oscillators is investigated. Being interested in mechanical structures, where the wavelength of the main dynamic phenomena is of the same order of magnitude of any element of the chain, discrete nonlinear periodic models governed by second order nonlinear difference equations are studied.

Monocoupled periodic systems of infinite extent with material nonlinearities have been addressed in [Vakakis and King, 1995]. Two different asymptotic approaches have been devised for studying standing (stop-bands) and traveling (pass-bands) waves; amplitude dependent frequency thresholds bounding nonlinear propagation and attenuation zones have been found. In [Davies and Moon, 1996] an array of elastic oscillators coupled through buckling sensitive elastica has been addressed both numerically and experimentally. Localized modes in chains of oscillators with cubic nonlinearities have been studied in [Manevitch, 2001] through an asymptotic approach. In [Chakraborty and Mallik, 2001], harmonic wave propagation in weakly nonlinear periodic structures made up of chains of masses joined by nonlinear springs has been investigated through a perturbation expansion of the propagation constant; bounding frequencies of propagation zones as well as nonlinear normal modes of finite chains have been determined. More recently, wave attenuation caused by weak linear/nonlinear damping has been addressed in [Marathe and Chatterjee, 2006], where the method of multiple scales is applied to the nonlinear map governing the dynamics of the periodic structure. Monocoupled chains of linearly coupled nonlinear oscillators have been studied in [Romeo and Rega, 2006] through a nonlinear map approach. According to this approach, conservative infinite chains of nonlinear oscillators can be investigated by means of nonlinear maps. The governing difference equations are regarded as symplectic nonlinear transformations relating the amplitudes in adjacent elements, by considering a dynamical system where the position plays the role of the discrete time [Hennig and Tsironis, 1999]. Thus, wave propagation becomes synonymous of stability: to find regions of propagating wave solutions is equivalent to find regions of linearly stable map solutions.

In this work mono-coupled finite chains with homogenous boundary conditions are considered in the backgrund of wave propagation results obtained for infinite chains. The non-linear normal modes of such multi-degree of freedom system correspond to periodic motions when all the coordinates cross their equilibrium position simultaneously and the associated frequencies are the so called non-linear natural frequencies. In this realm the preliminary, yet worthy, goal is to determine the free vibrations frequency-amplitude curves, and the associated nonlinear modes, as well as to discuss their relationship with the amplitude dependent frequency thresholds of the nonlinear propagation zone. The analysis is carried out for weak nonlineari-

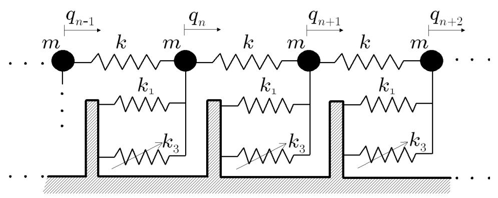

Figure 1. Monocoupled infinite nonlinear spring-mass chain.

ties through the multiple scales perturbation approach. Strong and weak linear coupling between the oscillators is discussed and the comparison between numerical and analytical results is presented.

2 Infinite chain of nonlinear oscillators: propagation regions

A mechanical model for an infinite chain of linearly-coupled nonlinear oscillators, schematically depicted in Figure 1, has been chosen in the form:

$$m\ddot{u}_n + k_1 u_n + k_3 u_n^3 + k(2u_n - u_{n-1} - u_{n+1}) = 0 \quad (1)$$

The equation of motion (1) is characterized by on-site cubic nonlinearity, as e.g. in [Manevitch, 2001], describing a chain of Hamiltonian oscillators. Periodic solutions of equation (1) are sought for by assuming the time harmonic solution $u_n = a_n \cos(\omega t)$ (harmonic balance with only the first harmonic), and setting $\alpha = \frac{m\omega^2 - k_1}{k} - 2$ and $\beta = -\frac{3k_3}{4k}$, the following second-order difference equation for the stationary amplitude is obtained

$$(\alpha + \beta a_n^2)a_n + a_{n+1} + a_{n-1} = 0 \qquad (2)$$

Equation (2), relating the amplitudes a in adjacent chain sites $n-1$, n and $n+1$, can be rewritten in matrix form as $\mathbf{a}_{n+1} = \mathbf{T}(a_n)\mathbf{a}_n$, where $\mathbf{T}(a_n)$ is the nonlinear transfer matrix. In the linear case, $\mathbf{T}$ represents a symplectic linear transformation and its reciprocal eigenvalues λ satisfy $\lambda_1\lambda_2 = 1$. As well known, such eigenvalues govern the stationary wave transmission properties: if the eigenvalues lie on the unit circle, then free waves propagate harmonically without attenuation (pass band, $\mathbf{P}$); if the eigenvalues are real, then free waves decay without oscillations (stop band, $\mathbf{S}$). In the more general nonlinear case, $\mathbf{T}(a_n)$ belongs to the class of area preserving maps such that $\det(\mathbf{DT}(a_n)) = 1$, where $\mathbf{DT}$ is the Jacobian or tangent map with reciprocal eigenvalues. Therefore, in order to study the stationary wave transmission properties of the one-dimensional nonlinear chain (1) of lenght N, it is convenient to rely on the eigenvalues of the linearized map equations in the neighborhood of an orbit ranging from (a_0, a_1) to (a_{N-1}, a_N). Indeed, according to [Hennig and Tsironis, 1999], the transformation $\mathbf{a}_{n+1} = \mathbf{T}(a_n)\mathbf{a}_n$ can be considered as a dynamical system where the chain index n plays the role of discrete time, so that the analysis of the transmission properties is equivalent to the stability analysis of the orbits. The linear stability of a given orbit is investigated by introducing a small complex-valued perturbation v_n; linearizing the map equations, a second-order difference equation for the perturbation is obtained leading to the two-dimensional Jacobian

$$\mathbf{DT} = \begin{bmatrix} -\alpha - 3\beta a_n^2 & -1 \\ 1 & 0 \end{bmatrix} \qquad (3)$$

The interest lies in the linear stability of spatially periodic orbits $a_{n+q} = a_n$ with cycle length q. The eigenvalues of $\mathbf{DT}$ are determined by its trace, so the stability of period-q orbits is described by $tr(\mathbf{DT}^q)$. If the eigenvalues lie on the unit circle, then stable elliptic periodic cycles or oscillating solutions (pass band, $\mathbf{P}$) occur; if the eigenvalues are real, then unstable hyperbolic periodic cycles or exponentially increasing solutions (stop band, $\mathbf{S}$) occur [Hennig and Tsironis, 1999]. For period-1 orbits the curves bounding the propagation regions, where the eigenvalues lie on the unit circle, can be determined by the condition $|tr(\mathbf{DT})| = 2$. Having set $a_{n+1} = \tilde{x}_{n+1}$ and $a_n = \tilde{y}_{n+1}$ and introduced the change of variables $(\tilde{x}, \tilde{y}) \rightarrow (x/\sqrt{\beta}, y/\sqrt{\beta})$, such boundaries are given by

$$\begin{aligned} r &:= \{(x, \alpha) \mid 3x^2 + \alpha + 2 = 0\} \\ s &:= \{(x, \alpha) \mid 3x^2 + \alpha - 2 = 0\} \end{aligned} \qquad (4)$$

and are shown in Figure 2a in the x-positive half-plane. The curves r and s represent hyperbolic ($\lambda_1 = \lambda_2 = 1$) and reflection hyperbolic ($\lambda_1 = \lambda_2 = -1$) boundaries, respectively. In Figure 2b further curves t_i, lying inside the pass band region, are depicted; they are determined by satisfying the condition $|tr(\mathbf{DT}^q)| = 2$ for $q = 4$ and their number depends on the periodicity of the orbit, i.e. t_i with $i = 1, \ldots, q-1$. While the curves r are always hyperbolic boundaries, the curves s are either hyperbolic with reflection boundaries, for q odd, or hyperbolic boundaries, for q even. Whenever a period-q orbit crosses a curve t_i it temporarily loses its stability or, equivalently, does not propagate, through either a saddle-node or a period-doubling bifurcation for i even or i odd, respectively. As expected, the nonlinearity ($\beta \neq 0$) implies a propagation region depending on the amplitude of oscillations $x = \tilde{x}\sqrt{\beta}$ (see Figure 2), in contrast to the linear case, where the propagation region is given by $|\alpha| \leq 2$. As thoroughly described in [Romeo and Rega, 2006], period-1 and period-4 orbits, representing the fixed points of $\mathbf{T}$ and $\mathbf{T}^4$, respectively, are determined as

$$\begin{aligned} &\text{Period-1}: \quad x = y = \pm\sqrt{-2-\alpha} \\ &\text{Period-4}: \quad x = y = \pm\sqrt{-\alpha} \end{aligned} \qquad (5)$$

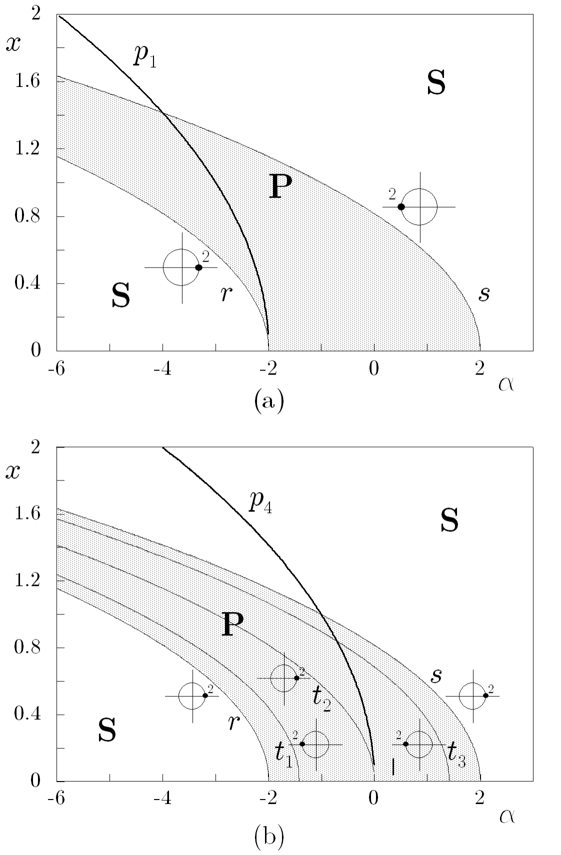

Figure 2. Propagation region of period-q orbits: a) $q = 1$; b) $q = 4$.

and are superimposed in Figures 2a and 2b, respectively. It can be noticed that, regardless of the periodicity q, the bounded orbits region coincides with that of the period-1 case whose boundaries are given by the curves of equations (4).

3 Finite chains: nonlinear frequencies and modes

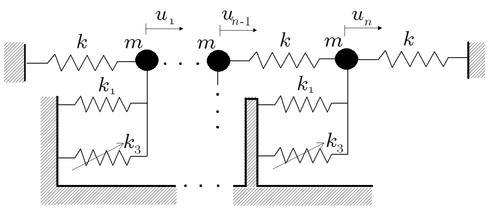

Figure 3. Monocoupled finite nonlinear spring-mass chain.

In this section we consider a finite chain composed by N mono-coupled weakly nonlinear oscillators having both ends fixed; the chain model is derived from equation (1) and it is sketched in Figure 3. The governing equations of motion can be written in the compact form

$$\mathbf{I}\ddot{\mathbf{u}} + \mathbf{K}\mathbf{u} + \hat{\beta}\mathbf{n} = \mathbf{0} \tag{6}$$

where $\mathbf{u} = (u_1, u_2, \ldots, u_N)^T$, $\mathbf{n} = (u_1^3, u_2^3, \ldots, u_N^3)^T$, **I** and **K** are the NxN identity and stiffness matrices, respectively; the latter is a tridiagonal matrix of the form

$$\mathbf{K} = \begin{bmatrix} \alpha_1 & -\alpha_2 & 0 & 0 & 0 \\ -\alpha_2 & \alpha_1 & -\alpha_2 & 0 & 0 \\ 0 & \cdot & \cdot & \cdot & 0 \\ 0 & 0 & -\alpha_2 & \alpha_1 & -\alpha_2 \\ 0 & 0 & 0 & -\alpha_2 & \alpha_1 \end{bmatrix} \tag{7}$$

and the parameters are: $\alpha_1 = (k_1 + 2k)/m$, $\alpha_2 = k/m$ and $\hat{\beta} = k_3/m$; the first and last row of **K** take into account the boundary conditions. The weak cubic nonlinearity allows us to assume a series expansion of the solution as:

$$\mathbf{u} = \varepsilon\mathbf{u}_1 + \varepsilon^3\mathbf{u}_3, \quad \frac{d}{dt} = d_0 + \varepsilon^2 d_2 + \ldots \tag{8}$$

with $d_k = \partial/\partial t_k$ and $t_k = \varepsilon^k t$ ($k = 0, 2, \ldots$), so that the perturbation equations read

$$\begin{aligned} \varepsilon: &\quad \mathbf{I}\ddot{\mathbf{u}}_1 + \mathbf{K}\mathbf{u}_1 = 0 \\ \varepsilon^3: &\quad \mathbf{I}\ddot{\mathbf{u}}_3 + \mathbf{K}\mathbf{u}_3 = -\hat{\beta}\mathbf{n}_1 - 2d_0d_2\mathbf{u}_1 \end{aligned} \tag{9}$$

where $\mathbf{n}_1 = (u_{11}^3, u_{12}^3, \ldots, u_{1N}^3)^T$. The order ε solution of equation (9_1) can be put in the form $\mathbf{u}_1 = \sum_{j=1}^{N} \mathbf{u}_{1j}$, where

$$\mathbf{u}_{1j} = A_j \boldsymbol{\phi}_j e^{i\omega_j t} + c.c. \tag{10}$$

with $\boldsymbol{\phi}_j = (\phi_{j1}, \phi_{j2}, \ldots, \phi_{jN})^T$ being the j-th orthonormal linear mode and ω_j the corresponding linear frequency. By substituting expression (10) in the order ε^3 equations (9_2) we get, for each higher-order modal contribution,

$$\begin{aligned} \mathbf{I}\ddot{\mathbf{u}}_{3j} + \mathbf{K}\mathbf{u}_{3j} = \Big(&-\hat{\beta}A_j^3\boldsymbol{\xi}_j e^{3i\omega_j t} - \\ &3\hat{\beta}A_j^2\bar{A}_j\boldsymbol{\eta}_j e^{i\omega_j t} - 2i\omega_j\boldsymbol{\phi}_j A_j' e^{i\omega_j t}\Big) + c.c. \end{aligned} \tag{11}$$

with the vectors $\boldsymbol{\xi}_j = (\phi_{j1}^3, \phi_{j2}^3, \ldots, \phi_{jN}^3)^T$ and $\boldsymbol{\eta}_j = (\phi_{j1}^2\bar{\phi}_{j1}, \phi_{j2}^2\bar{\phi}_{j2}, \ldots, \phi_{jN}^2\bar{\phi}_{jN})^T$ including the mode nonlinearities. In the non-internally resonant case, the solvability condition for the j-th mode yields

$$\boldsymbol{\phi}_j^T(-3\hat{\beta}A_j^2\bar{A}_j\boldsymbol{\eta}_j - 2i\omega_j A_j'\boldsymbol{\phi}_j) = 0 \tag{12}$$

entailing

$$A_j' = -\frac{3\hat{\beta}A_j^2\bar{A}_j\boldsymbol{\phi}_j^T\boldsymbol{\eta}_j}{2i\omega_j\boldsymbol{\phi}_j^T\boldsymbol{\phi}_j} \tag{13}$$

Taking equation (13) into account, equation (11) reads

$$\mathbf{I}\ddot{\mathbf{u}}_{3j} + \mathbf{K}\mathbf{u}_{3j} = -\hat{\beta} A_j^3 \boldsymbol{\xi}_j e^{3i\omega_j t_0} + c.c. \qquad (14)$$

and a particular solution of the latter can be found via the method of undetermined coefficients by letting

$$\mathbf{u}_{3j} = \boldsymbol{\gamma}_j A_j^3 e^{3i\omega_j t_0} + c.c. \qquad (15)$$

where $\boldsymbol{\gamma}_j = (\gamma_{j1}, \gamma_{j2}, \ldots, \gamma_{jN})^T$. By substituting (15) into (14) a set of algebraic equations for the $\boldsymbol{\gamma}_j$ is obtained:

$$\left(\mathbf{K} - 9\,\omega_j^2 \mathbf{I}\right) \boldsymbol{\gamma}_j = -\hat{\beta} \boldsymbol{\xi}_j + c.c. \qquad (16)$$

Once the vector $\boldsymbol{\gamma}_j$ is determined, the j-th modal response is obtained as

$$\mathbf{u}_j = \varepsilon A_j \boldsymbol{\phi}_j e^{i\omega_j t_0} + \varepsilon^3 \boldsymbol{\gamma}_j A_j^3 e^{3i\omega_j t_0} + c.c. \qquad (17)$$

By writing A_j in the polar form $A_j = 1/2 a_j e^{i\theta_j}$, substituting into the solvability equation (12) and separating real and imaginary parts we obtain

$$a_j' = 0 \qquad \vartheta_j' = \frac{3\,\hat{\beta} a_j^2 \boldsymbol{\phi}_j^T \boldsymbol{\eta}_j}{8\,\omega_j} \qquad (18)$$

where equation (18_2) represents the natural frequencies corrections. Moreover, the solution (17), reabsorbing the ε, can be expressed in trigonometric form as follows

$$\mathbf{u}_j = a_j \boldsymbol{\phi}_j \cos(\omega_j t_0 + \theta_j) + \frac{1}{4} a_j^3 \boldsymbol{\gamma}_j \cos(3\,\omega_j t_0 + 3\,\theta_j) \qquad (19)$$

In view of the numerical investigation presented in Section 4, where the frequency-amplitude curves of finite chains will be shown against the propagation region of the infinite chain, the parameter $\mu = k_1/k$ is introduced. It allows to investigate the effect of the ratio between the on-site (k_1) and the coupling (k) linear stiffnesses on the wave propagation. Aiming at analysing the effect of μ, the propagation regions described in Section 2 are herein represented in the μ-ω-a space (Figure 4a) and its μ-ω plane projection (Figure 4b). In particular the propagation region lies between the upper and lower bounding surfaces given by the corresponding version of equations (4). It is seen that, as μ increases, the propagation region shrinks since the effect of coupling between the oscillators of the chain becomes weaker and weaker in absolute or relative sense.

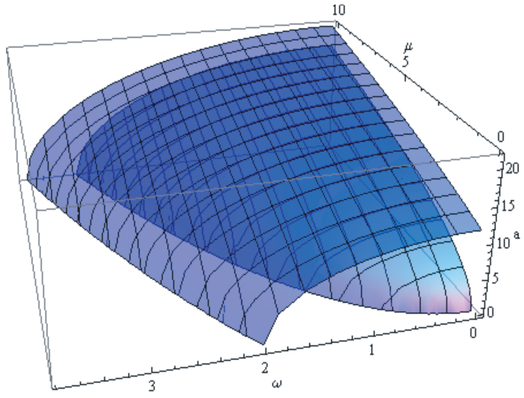

(a)

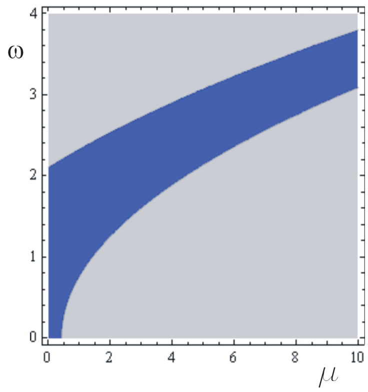

(b)

Figure 4. Propagation region vs coupling stiffness ratio ($\hat{\beta}$=0.01). a) Amplitude dependent propagation region in the μ-ω-a space; b) propagation region in the μ-ω plane.

4 Numerical investigations

Results pertaining to instances of finite chains as sketched in Figure 3 are presented in this section. Chains of 15 elements are considered and the frequency-amplitude relation governing nonlinear free vibrations is evaluated based on the natural frequencies corrections given by equation (18_2) having set $\hat{\beta} = 1$. In Figure 5 such frequency-amplitude curves are presented against the nonlinear propagation regions of the corresponding infinite chain. As expected, for small amplitude oscillations all the natural frequencies fall within the passing band. Figure 5a and 5b refer to chains characterized by strong ($\mu = 0.1$) and weak ($\mu = 10.0$) coupling between the oscillators. The propagation regions shrinking, previously shown in Figure 4, entails the increasing of modal density as the coupling becomes weaker.

The modal response given by equation (19) is also investigated. In Figure 6 the nonlinear correction of the mode shapes as the amplitude increases is shown for the first (6a) and the eighth (6b) modes for the same five amplitude levels. Analysis of the other modes lead to infer that the nonlinear correction becomes weaker

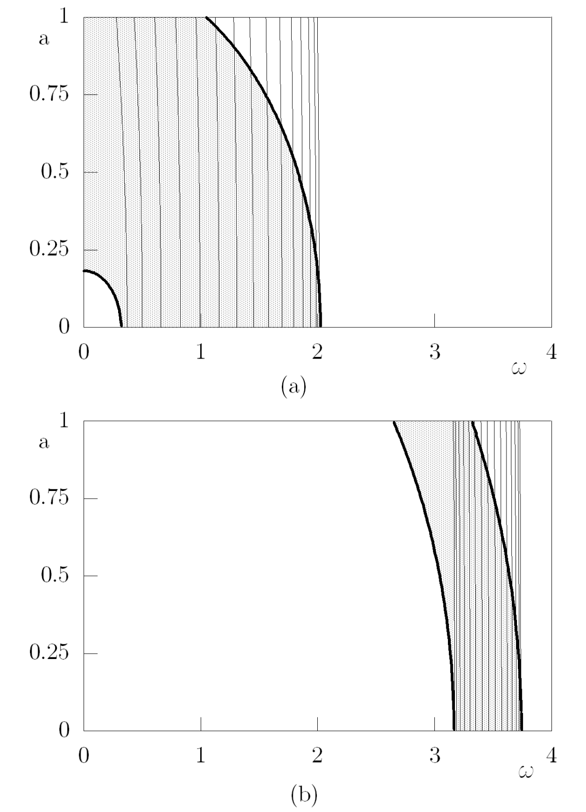

Figure 5. Chain of 15 nonlinear oscillators: frequency-amplitude relations against the nonlinear propagation region ($\hat{\beta}$=1). a) $\mu = 0.1$; b) $\mu = 10.0$.

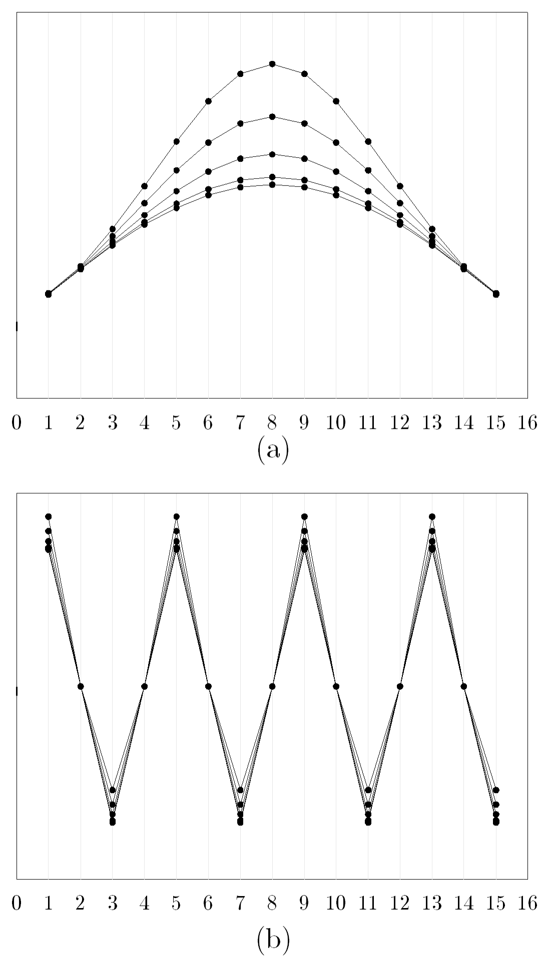

Figure 6. Chain of 15 nonlinear oscillators: nonlinear correction of the mode shapes as the amplitude increases. a) First mode; b) eighth mode.

as the mode number increases. Figures 7 and 8 show the time evolution of the first and eighth mode, respectively. In particular, the linear cases are shown in Figures 7a and 8a while the nonlinear ones are represented in 7b and 8b. The modes are sampled at equal time intervals, chosen according to the relevant periods. Therefore the expected anharmonic response in presence of nonlinearity can be noticed from the loss of symmetry with respect to the resting position. As shown in Figures 6b and 8, the eighth mode turns out to be a spatially period-4 solution of the considered finite chain. This circumstance occurs for any fixed-fixed chain (Figure 3) with N oscillators, for the $(N+1)/2$-th mode, with N odd and greater than 1. Thus, the eighth frequency-amplitude approximated curve can be compared with the analytical one for the infinite chain given by equation (5b). Such comparison provides with the frequency differences (%) reported in Figure 9 for increasing response amplitude and $\hat{\beta}$=0.5.

5 Conclusions

Frequency-amplitude relations and nonlinear modes in finite, fixed-fixed chains of weakly nonlinear oscillators, have been built through the multiple scale perturbation approach. These results have been considered against the nonlinear propagation regions of the infinite chain. The latter have been studied based on the (space/time) analogy of the linear stability analyses of the relevant maps, that provided analytically both the boundaries of pass-band regions and the periodic orbits. The frequency-amplitude curves obtained for the finite chain highlighted that for small amplitude oscillations all the natural frequencies fall within the nonlinear passing band. Moreover a good agreement between the spatial period-4 solution obtained from the perturbation analysis and the analytical one, given by the map approach, was found. Since only on-site nonlinearities were taken into account it is expected that different boundary conditions will not affect the pursued treatment and the overall conclusions whilst certainly implying quantitative modifications of the results.

Future work will address the possible correlation between the stability analysis of the perturbation spatially periodic solutions and the wave propagation analysis of the infinite chain.

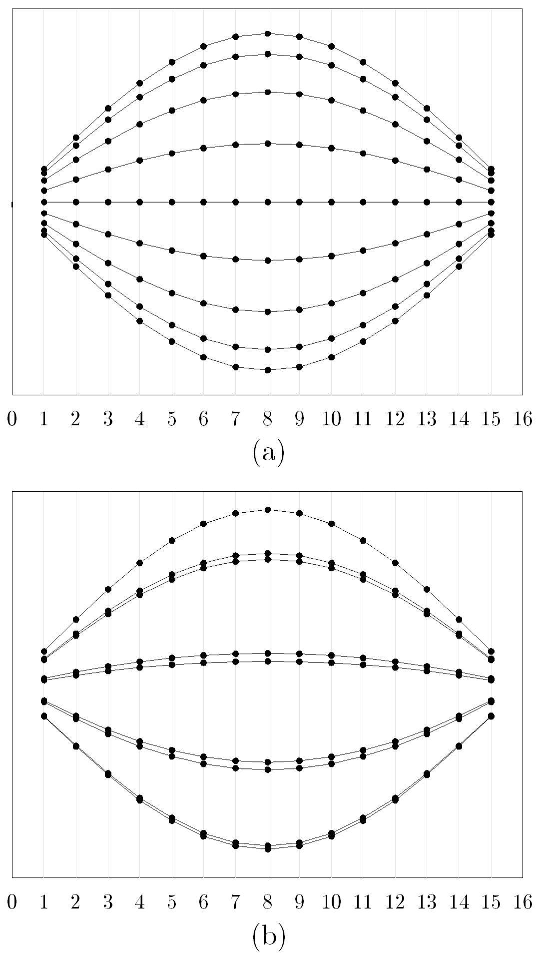

Figure 7. Chain of 15 nonlinear oscillators: first mode time evolution. a) Linear ; b) nonlinear.

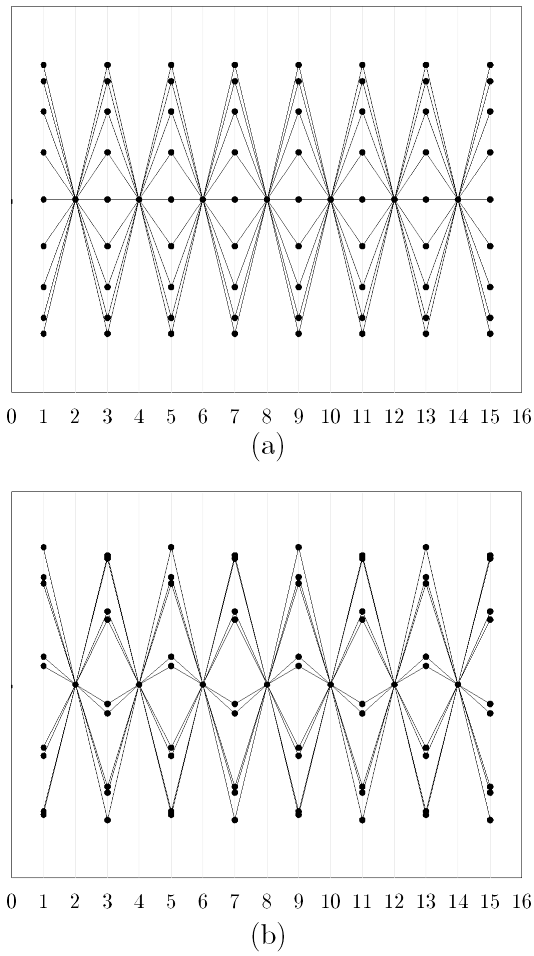

Figure 8. Chain of 15 nonlinear oscillators: eighth mode time evolution. a) Linear ; b) nonlinear.

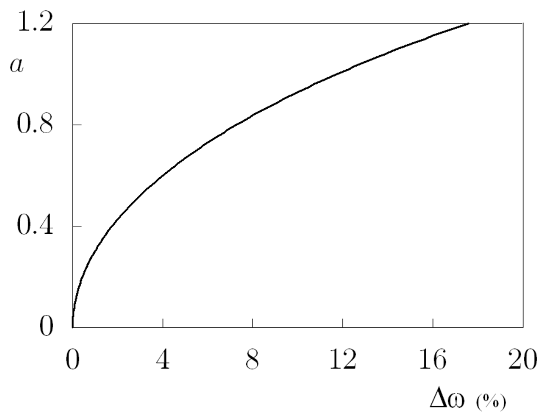

Figure 9. Frequency difference (%) with increasing response amplitude between the spatially period-4 analytical solution of the infinite chain and the corresponding normal mode of the finite chain of 15 oscillators ($\hat{\beta}$=0.5).

References

Vakakis A.F. and King M.E., (1995). Nonlinear wave transmission in a mono-coupled elastic periodic system. *J. of Acoust. Soc. Am.*, **98** , pp. 1534–1546.

Davies, M.A. and Moon, F.C. (1996). Transition from soliton to chaotic motion following sudden excitation of a nonlinear structure. *J. of Applied Mechanics*, **63** , pp. 445–449.

Manevitch, L.I. (2001). The description of localized normal modes in a chain of nonlinear coupled oscillators using complex variables. *Nonlinear Dynamics*, **25** , pp. 95–109.

Chakraborty, G. and Mallik, A.K. (2001). Dynamics of a weakly non-linear periodic chain. *Int. J. of Nonlinear Mechanics*, **36** , pp. 375-389.

Marathe, A. and Chatterjee, A. (2006). Wave Attenuation in Nonlinear Periodic Structures Using Harmonic Balance and Multiple Scales.*J. of Sound and Vibration*, **289**, pp. 871-888.

Romeo, F. and Rega, G. (2006). Wave propagation properties in oscillatory chains with cubic nonlinearities via nonlinear map approach. *Chaos Solitons & Fractals*, **27**, pp. 606–617.

Hennig, D. and Tsironis, G.P. (1999). Wave transmission in nonlinear lattices. *Physics Reports*, **307**, pp. 333–432.